Available online at www.sciencedirect.com
SCIENCE DIRECT®
Thermochimica Acta 416 (2004) 11–16
thermochimica acta
www.elsevier.com/locate/tca

Thermal study of copper adsorption on montmorillonites

Zhe Ding*, Ray L. Frost

Inorganic Materials Research Program, School of Physical and Chemical Sciences, 2 George Street, GPO Box 2434, Brisbane, Qld 4001, Australia

Available online 20 April 2004

Abstract

Copper was adsorbed onto Ca-exchanged montmorillonite (Cheto clay) under basic conditions. Differential thermogravimetric analysis (DTGA) combined with mass spectroscopy (MS) was employed as the principal technology to study the distributions and structures of adsorbed copper species on Cheto clay. The results showed that the original Cheto clay was easily rehydrated. After copper adsorption, a step-by-step replacement of hydrated calcium ions by copper–ammonia complex was observed through the gradual decrease of the first DTGA dehydration peak intensity with the increasing copper loading amount. Compared with the original Cheto clay, copper-loaded samples showed new DTGA peaks assigned to NH_3 and N_2O. The presence of N_2O peak suggested that the loaded copper species were in agglomerated copper oxide form, which dispersed well over the edge and external surface of the clay layers.

Keywords: Copper adsorption; Montmorillonite; TGA–MS analysis; Controlled rate thermal analysis

1. Introduction

Adsorption of metal ions onto clay minerals is an interesting topic and has been studied extensively. Both metal ions and clays are common components in nature and such study would provide useful information on the state of the metal ions and how they distribute in the environment. In addition, it can also enrich the knowledge of the adsorption process for the environmental remediation of the polluted heavy metal ions in water.

From our point of view, copper is of particular interest, because of its catalytic performance in the reactions such as wet air oxidation (WAO) [1–6] for wastewater treatment and selective catalytic reduction (SCR) of NO_x [7–9]. Copper has been loaded onto different supports and used as catalysts in these reactions. The most explored supporting materials are zeolite [9], alumina [2,3] and titania [8]. There are few reports using clay as supports for such applications and information about the structure of the different clay supported copper phases is rare. Considering the large deposits of clay minerals, it will be economic favourable to use clay as catalyst supports. The previous studies showed the promising catalytic performance for copper loaded pillared clays in WAO [10,11] and SCR [12–14] reactions. In these works, before copper adsorption, clay was modified by pillaring process to enhance the surface area and porosity [13,15,16]. The catalytic reaction results showed that the amount and state of the adsorbed copper species was critical for the catalytic activities. Therefore, it is worthwhile to apply raw clays as supporting materials. The focus of this study is to investigate the adsorption of copper onto clays and their structures under different synthesis concentrations. For the first time, combined DTGA–MS technique was used to distinguish the different locations of the adsorbed copper species on the clay surface.

2. Experimental

2.1. Sample preparation

The starting clay material was Cheto montmorillonite (from Clay Minerals Repository, University of Missouri-Columbia). It was mainly Ca-exchanged montmorillonite and used as received without any additional treatment.

Copper adsorption was conducted under basic conditions. To 0.01 M of copper nitrate solution, ammonia was added to adjust the pH to 12. Various amounts of this copper solution was added to 5 wt.% of clay suspension with Cu/clay ratios of 0.2, 0.5 and 1 mmol/g, respectively. The resulting

* Corresponding author. Tel.: +61-7-3864-1220; fax: +61-7-3864-1804.
E-mail address: z.ding@qut.edu.au (Z. Ding).

0040-6031/$ – see front matter © 2003 Elsevier B.V. All rights reserved.
doi:10.1016/j.tca.2003.11.037

suspension was kept on stirring for 18 h, followed by separation, washing and drying slowly at 80 °C. Thus obtained samples were labelled as Cu/Cheto-*n*, where $n = 1$, 2, and 3 to represent different Cu/clay ratios.

2.2. Characterisation

DTGA–MS was conducted on TA® Instruments Thermogravimetric Analyser (TGA, Q500) equipped with an evolved gas analysis (EGA) furnace, which was connected to a Quadrupole Mass Spectrometer (PFEIFFER, QMS 200 Prisma) through a 1/8 in., in diameter, transfer line. Nitrogen was used as the purging gas and the flow rate was controlled precisely at 80 ml/min. Around 50 mg of sample powders were loaded onto platinum sample pan and the analysis was performed under two conditions. A normal ramp procedure was used for condition I. Sample was preheated to 30 °C and isothermal for 10 min, then it was heated to 900 °C at a heating rate of 4 °C/min. A controlled rate thermal analysis (CRTA) was used for condition II. Sample was heated to 900 °C at a high-resolution heating rate of 10 °C/min, where the heating rate was dynamically and continuously modified according to the changes in the rate of the sample weight loss.

X-ray diffraction (XRD) patterns of the samples were colleted on ENRAF NONIUS DELFT DIFFRACTIS 583, using Co Kα radiation. Sample powders were calcined at 400 °C for 5 h and XRD measurements were performed on both the calcined and freshly prepared samples. Each XRD scan was obtained at a speed of 1°/min with step size of 0.02°.

X-ray photoelectron spectroscopy (XPS) analysis was conducted on a PHI model 560 XPS/SAM/SIMS I multitechnique surface analysis system. The X-ray source was provided by the monochromatic Mg Kα radiation, which was operated at 15 kV. Powders were loaded onto sample holder by double face sticky tape. Since the thickness of single clay layer is around 9.8 Å and XPS can detect surface information within depth of 60 Å. Therefore, the element concentrations obtained from XPS measurement were treated as the bulk concentrations.

3. Results and discussion

Table 1 gives the *d*-spacings, calculated from the XRD analysis, for the original Cheto clay and different Cu/Cheto-*n* samples before and after calcination. It is clear that for Cheto clay, there is little variation in the *d*-spacing after calcination, 1.58 nm compared with 1.55 nm. This indicates that Cheto clay rehydrates easily. After copper adsorption, there is a decrease of the *d*-spacings for both samples before and after calcination. Furthermore, there is not much difference among the three Cu/Cheto-*n* samples, except that the Cu/Cheto-1 shows slightly higher *d*-spacing. Contrary to what happened to the original Cheto clay, a general decrease of the *d*-spacing after calcination is observed, which implies that Ca is replaced by Cu species and the latter does not rehydrate after being calcined. One would expect that these exchanged Cu species sit in-between the clay layers. However, considering the thickness of the single clay layer, which is 0.98 nm, it is clear that there is no layer expansion after copper loading. A slight higher *d*-spacing for Cu/Cheto-1 might come from the copper species sit in-between the layers, or might come from the incomplete exchanging of Ca by Cu. Apart from the characteristic peaks assigned to montmorillonite clay, no other peaks are detected for any types of copper crystallite phases from XRD study.

The bulk element concentrations determined from XPS analysis are also listed in Table 1. It is seen that the copper loading amount is proportional to the starting Cu/clay ratio during the synthesis and it seems would reach a plateau if further increase the Cu/clay ratio to higher than 1 mmol/g. In addition, for Cu/Cheto-1, there is still 2.0 wt.% CaO after copper exchanging, which is reduced to 0.55 wt.% for Cu/Cheto-2. Therefore, the higher *d*-spacing in XRD analysis for Cu/Cheto-1 compared with the other two samples is more likely coming from the rehydration of those un-exchanged Ca.

The normal ramping DTGA–MS results for original Cheto clay and Cu/Cheto-*n*, using Cu/Cheto-2 as representative, are illustrated in Figs. 1 and 2, respectively.

From Fig. 1, it is seen that the starting Cheto clay has two main weight loss regions: (i) below 200 °C, and (ii) between 500 and 700 °C. The on-line MS analysis shows that only water, mass 18 and 17, is generated during the sample heating and the MS data follows the same trend as that of DTGA data. Therefore, Cheto clay has two dehydration peaks centred at 63 and 125 °C, region (i), and one broad dehydroxylation peak centred at 608 °C, region (ii). Such a result is typical for montmorillonite clays, which upon heating, surface adsorbed water is lost first. Further heating will cause breaking of the structural hydroxyl groups,

Table 1
d-spacings and bulk element concentrations for different samples

Sample	*d*-spacing (nm)		SiO_2 (wt.%)	Al_2O_3 (wt.%)	MgO (wt.%)	CaO (wt.%)	CuO (wt.%)
	Fresh	400 °C					
Cheto	1.55	1.58	62	21	6.5	2.7	0
Cu/Cheto-1	1.27	1.01	63	19	5.4	2.0	1.5
Cu/Cheto-2	1.23	0.99	63	20	5.6	0.55	4.0
Cu/Cheto-3	1.23	0.99	64	21	4.7	0	5.3

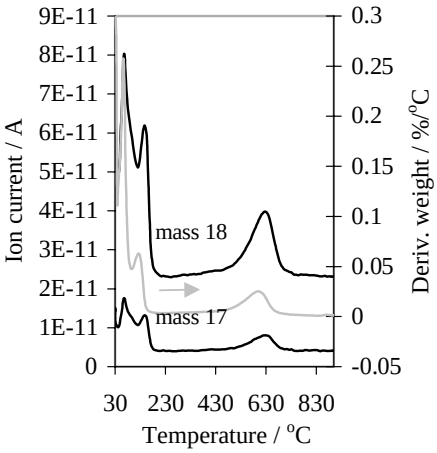

Fig. 1. DTGA–MS (analysis condition I) results for original Cheto clay.

leading to the dehydroxylation peak at higher temperature. It is believed that the dehydroxylation process is partially non-reversible, where the layered structure collapses. However, adsorption/desorption of water is reversible. From Fig. 1, it is clear that the dehydroxylation only happens when temperature is over 500 °C. This supports the results obtained from XRD analysis that the calcination temperature (400 °C) is not high enough to destroy the layered structure and the Cheto clay easily rehydrated.

For the Cu/Cheto-*n* samples, as shown in Fig. 2, four main weight loss regions are observed: (i) below 150 °C, (ii) between 150 and 350 °C, (iii) between 350 and 700 °C, and (iv) between 800 and 870 °C. In addition, more signals have been picked up during the on-line MS analysis, including mass 16, 17, 18, 32, and 44. Because the copper exchanging was conducted under basic condition by adding ammonia, the major exchanging species would be $Cu(NH_3)_4^{2+}$. Therefore, in MS results, mass 16 is assigned to ammonia,

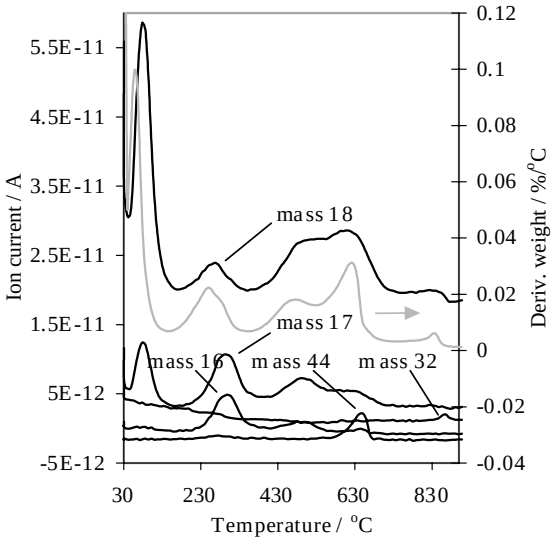

Fig. 2. DTGA–MS (analysis condition I) results for Cu/Cheto-2.

mass 18 is coming from water, while mass 17 can be either water or ammonia. Mass 32 is oxygen, which appears at fairly high temperature, indicating the reconstructing of the adsorbed copper species. The presence of mass 44 is not anticipated. The first thought is to assign it to CO_2, which is coming from the organic impurity in Cheto clay. However, mass 44 was not detected in the MS analysis for original Cheto clay, which excludes such possibility. Considering that the TGA analysis was performed under the nitrogen condition, it is likely that mass 44 is not a result of the pure weight loss, but a reaction between the sample and nitrogen:

$$2CuO + N_2 \rightarrow Cu_2O + N_2O \quad (1)$$

or

$$CuO + N_2 \rightarrow Cu + N_2O \quad (2)$$

Therefore, mass 44 is assigned to N_2O. Combine MS data with DTGA data, it is proposed that Cu/Cheto-2 undergoes the following steps during heating. In region (i), mainly water is desorbed with a dehydration peak centred at 65 °C. More water is released in region (ii), centred at 250 °C, and region (iii), centred at 510 and 610 °C. Compared with the original Cheto clay, the dehydration peak at 125 °C disappears and Cu/Cheto-2 has new dehydration peaks at 250 and 510 °C, which are believed to be more related to the water associated with the adsorbed copper species. In addition, Cu/Cheto-2 has the similar dehydroxylation peak (610 °C) as that of Cheto clay. In the same regions (ii) and (iii), ammonia is also released with peaks centred at 300 and 470 °C. Therefore, adsorbed copper species are located on at least two different types of sites. Furthermore, in the end of region (iii), N_2O is produced, with peak centred at 650 °C. In region (iv), only oxygen is released with peak centred at 865 °C.

A comparison of DTGA curves for different Cu/Cheto-*n* samples is given in Fig. 3. It is seen that Cu/Cheto-1 and 3 have the similar DTGA pattern as that of Cu/Cheto-2. In region (i), Cu/Cheto-1 shows the highest dehydration peak, followed by Cu/Cheto-2 and Cu/Cheto-3. In addition, Cu/Cheto-1 has a shoulder around 130 °C, similar position as the second dehydration peak for the original Cheto clay. As

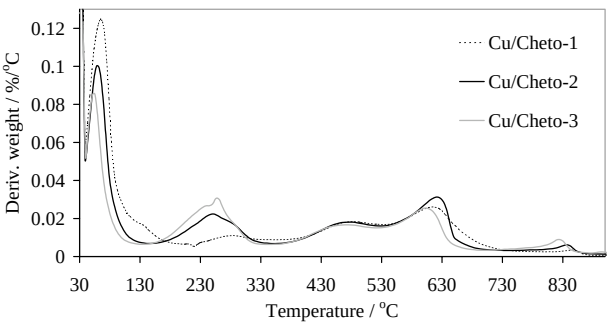

Fig. 3. Comparison of DTGA (analysis condition I) results for different Cu/Cheto-*n* samples.

discussed before, Cheto clay has exchangeable hydrated calcium on it. After treated with copper solution, those hydrated calcium ions are replaced by copper ions. Since copper ions were surrounded by ammonia, after copper exchanging, less water is adsorbed onto clay surface. Therefore, the first dehydration peak intensity decrease in Fig. 3 clearly reflects the step-by-step exchanging of calcium ions by copper ions. The exceptional shoulder for Cu/Cheto-1 is also coming from the least exchanging extent for Cu/Cheto-1, which agrees well with the above XRD and XPS results.

The weight loss in region (ii) is dominated by ammonia. Although clay itself also adsorbs ammonia, it is believed that the ammonia is introduced into clay structure mainly through adsorbed $Cu(NH_3)_4^{2+}$ complex. If this is true, the amount of ammonia desorbed during TGA analysis should be closely related to the amount of copper loaded. From Fig. 3, it is seen that in this region, the peak intensities follow the trend Cu/Cheto-3 > Cu/Cheto-2 > Cu/Cheto-1, which is the same order as those of the copper concentrations listed in Table 1. Therefore, DTGA results in regions (i) and (ii) demonstrate the replacement of the hydrated calcium ions by copper complex and the proportional relation between the exchange rate and the starting Cu/Cheto ratio.

The weight loss in region (iii) is more complicated, which is contributed from NH_3, H_2O and N_2O with the increase of the temperature. As discussed before, the simultaneous occurrence of NH_3 and H_2O around 500 °C indicates that copper complex is adsorbed on the different sites of clay surface. The peak intensity for NH_3 is much weaker in region (iii) than in region (ii), which implies that much less amount of copper complex adsorbed on this second type of sites. In addition, there is only a slight difference for the peak intensities among three samples, with the order of Cu/Cheto-1 > Cu/Cheto-2 > Cu/Cheto-3. Considering the presence of this peak at much higher temperature, it is assumed that the second type of adsorption sites (sites B) is located in-between the clay layers, while the first type of sites (sites A) is located on the edge or the external surface of the clay layer. During the sample preparation, most of the copper complex sits on the sites A with minor amount diffuses onto the sites B. When the sample is heated, the decomposition of the copper complex starts from sites A and further increasing the temperature results in the decomposition of the copper complex on sites B. It is not clear why the adsorption amount on sites B shows the reverse order as that on sites A, although the difference is not significant. One possible explanation is that with higher Cu/Cheto ratio, there are more copper complex adsorbed on the edge of the clay layer, which might block the entrance for the copper complex to diffuse into the gallery between layers. The former study showed that metal ion adsorption more likely happened on the edge of the clay layers when the solution had pH higher than 10 and particularly high background electrolyte concentration [17]. Since in this work, the copper exchange was conducted under pH of 12, edge adsorption would be favoured, which supports the above assumption. As for the dehydroxylation of clay structurally bonded hydroxyl groups, all three Cu/Cheto-*n* samples show dehydroxylation peak with similar position and intensity as that of the original Cheto clay. Therefore, the 2:1 dioctahedral clay structure is not affected by the copper-exchange. It is interesting to observe the N_2O peak during the TGA analysis. From Fig. 3, it is seen that the difference for this peak intensity among three samples is small, following the order of Cu/Cheto-2 > Cu/Cheto-1 > Cu/Cheto-3. As discussed before, it is proposed that this N_2O peak is a result of the kinetic reaction between the adsorbed copper species and carrier gas, nitrogen, but not a pure thermodecomposition. If this is correct, a normal ramping at 4 °C/min might not slow enough to let those copper species fully react with nitrogen and the result shown in Fig. 3 might be misleading.

To clarify this, TGA–MS analysis was conducted again under condition II. The results are illustrated in Figs. 4 and 5 for comparison. From Figs. 4(a) and 5(a), it is seen that DTGA curves for all three samples obtained under condition II follow the trends precisely as those obtained under condition I, except in region (iii) where N_2O is released. Fig. 5(a) shows apparently higher peak intensity for Cu/Cheto-2 than Cu/Cheto-1 and Cu/Cheto-3. The

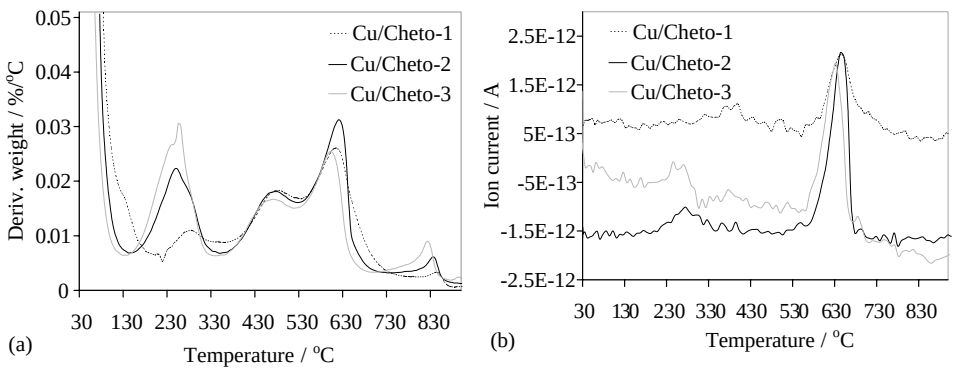

Fig. 4. DTGA–MS (analysis condition I) results for Cu/Cheto-*n* samples: (a) DTGA (replot on large scale); (b) MS for mass 44.

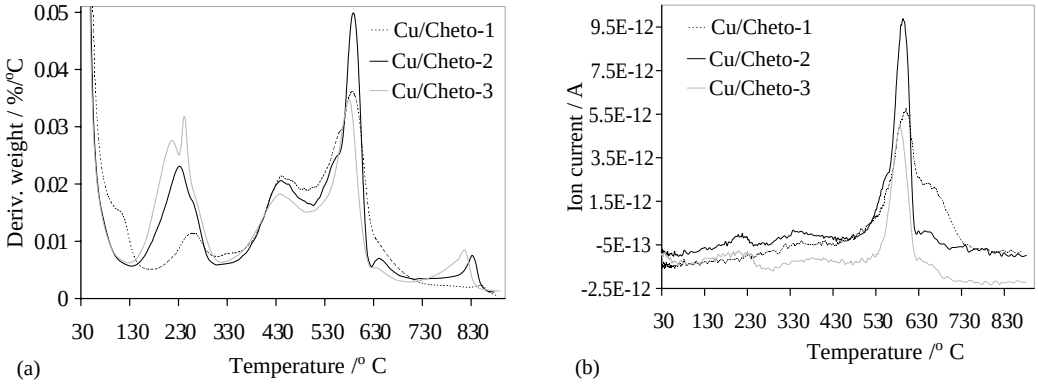

Fig. 5. DTGA–MS (analysis condition II) results for Cu/Cheto-*n* samples: (a) DTGA; (b) MS for mass 44.

corresponding MS comparison, Fig. 4(b) and 5(b), demonstrates the same discrepancy. Therefore, it is proved that N_2O is coming from the reaction between copper species and nitrogen. Furthermore, not all adsorbed copper species can join this reaction. The copper loading amount is in the order of Cu/Cheto-3 > Cu/Cheto-2 > Cu/Cheto-1. If all the copper species are involved in this reaction, one would expect to see the N_2O peak intensity following the same order, which is not the case in this study. As mentioned before, copper is absorbed on two types of sites. However, the structure of the adsorbed copper species has not been discussed. It was reported that with increase of pH, the structure of the adsorbed copper species would change from outer-sphere complex to inner-sphere monomer or multinuclear complex and finally to dimers under high pH [17,18]. It is believed that in this study, adsorbed copper has dimer or higher agglomerated structure. Depend on the starting Cu/Cheto ratio, the higher the ratio, the higher the extent of the agglomeration. There were also reports showed that with increasing of the heating temperature, migration of adsorbed copper from clay surface into octahedral structure happened [19,20]. However, this is more related to the isolated copper species and does not apply to this work. Therefore, in this study, most of the copper species present in agglomerated form on the edge or external surface of the clay layer. Since no signal for any crystallised copper phases was detected by XRD study, these agglomerated copper species disperse well over the clay surface. Fig. 5 shows the highest N_2O peak for Cu/Cheto-2, suggesting there is an optimum concentration, or agglomerated degree of copper for the reaction.

The weight loss in region (iv) is coming from oxygen, which does not exist in the original Cheto clay. The intensities for this peak follow the order of Cu/Cheto-3 > Cu/Cheto-2 > Cu/Cheto-1. Since similar peak was observed in the DTGA curve of the copper precursor, it is assigned to the reconstructing of the agglomerated copper species. The intensity change trend agrees well with the order of the copper concentration in the samples. This further supports the above discussion that higher copper concentration has higher tendency to agglomerate.

4. Conclusions

Copper adsorption on Cheto clay was conducted under the basic condition. The XRD results show that the original Cheto clay rehydrate easily. A clear step-by-step exchange of hydrated calcium by copper complex is presented through the DTGA–MS results. Two different types of copper adsorption sites (A and B) are determined in DTGA curves. Sites A, which are also the dominant one, locate on the edge or external surface of the clay layers. While sites B locate in-between the layers. Thermodecomposition of adsorbed copper complex happens first on sites A, corresponding to the DTGA peaks in region (ii). Further enhance the temperature results in the thermodecomposition of the adsorbed copper complex on sites B, corresponding to first part of the DTGA peaks in region (iii). With the help of MS, a kinetic reaction is distinguished from the pure thermodecomposition. The appearance of the N_2O and O_2 peaks shows that the adsorbed copper species are in agglomerated form and the higher the copper loading concentration, the higher the agglomerating extent. Although there is no exact picture of the copper structure, the appearance and intensity of N_2O can be used as a good indicator for the agglomerating status of copper species. DTGA–MS proved to be a valuable technique to study the adsorption of copper on clay samples and monitor the structure change during heating.

Acknowledgements

The authors thank the Inorganic Materials Research Program, School of Physical and Chemical Sciences, Queensland University of Technology, for the financial and infrastructure support. The Australian Research Council (ARC) is also gratefully acknowledged.

References

[1] F. Luck, Catal. Today 53 (1999) 81.
[2] A. Alejandre, F. Medina, A. Fortuny, P. Salagre, J.E. Sueiras, Appl. Catal. B: Environ. 16 (1998) 53.

[3] J. Yu, P.E. Savage, Appl. Catal. B: Environ. 28 (2000) 275.
[4] A. Alejandre, F. Medina, X. Rodriguez, P. Salagre, Y. Cesteros, J.E. Sueiras, Appl. Catal. B: Environ. 30 (2001) 195.
[5] P.M. Alvarez, D. McLurgh, P. Plucinski, Ind. Eng. Chem. Res. 41 (2002) 2147.
[6] P.M. Alvarez, D. McLurgh, P. Plucinski, Ind. Eng. Chem. Res. 41 (2002) 2153.
[7] B. Montanari, A. Vaccari, M. Gazzano, P. Kabner, H. Papp, J. Pasel, R. Dziembaj, W. Makowski, T. Lojewski, Appl. Catal. B: Environ. 13 (1997) 205.
[8] O.V. Komova, A.V. Simakov, V.A. Rogov, D.I. Kochubei, G.V. Odegova, V.V. Kriventsov, E.A. Paukshtis, V.A. Ushakov, N.N. Sazonova, T.A. Nikoro, J. Mol. Catal. A: Chem. 161 (2000) 191.
[9] X. Wang, W. Hou, X. Wang, Q. Yan, Appl. Catal. B: Environ. 35 (2002) 185.
[10] K. Bahranowski, M. Gasior, A. Kielski, J. Podobinski, E.M. Serwicka, L.A. Vartikian, K. Wodnicka, Clays Clay Miner. 46 (1998) 98.
[11] J. Barrault, C. Bouchoule, K. Echachoui, N. Frini-Srasra, M. Trabelsi, F. Bergaya, Appl. Catal. B: Environ. 15 (1998) 269.
[12] W. Li, M. Sirilumpen, R.T. Yang, Appl. Catal. B: Environ. 11 (1997) 347.
[13] R.T. Yang, N. Tharappiwattananon, R.Q. Long, Appl. Catal. B: Environ. 19 (1998) 289.
[14] M. Sirilumpen, R.T. Yang, N. Tharapiwattananon, J. Mol. Catal. A: Chem. 137 (1999) 273.
[15] K. Bahranowski, A. Kielski, E.M. Serwicka, E. Wisla-Walsh, K. Wodnicka, Microporous Mesoporous Mater. 41 (2000) 201.
[16] Z. Ding, J.T. Kloprogge, R.L. Frost, J. Porous Mater. 8 (2001) 273.
[17] J.D. Morton, J.D. Semrau, K.F. Hayes, Geochim. Cosmochim. Acta 65 (2001) 2709.
[18] S.P. Hyun, Y.H. Cho, S.J. Kim, P.S. Hahn, J. Colloid Interf. Sci. 222 (2000) 254.
[19] C. Mosser, L.J. Michot, F. Villieras, M. Romeo, Clays Clay Miner. 45 (1997) 789.
[20] H.P. He, J.G. Guo, X.D. Xie, J.L. Peng, Environ. Int. 26 (2001) 347.